

# Sintering of Aluminium Nitride: Particle Size Dependence of Sintering Kinetics

K. KOMEYA, H. INOUE

*Toshiba Research and Development Centre, Tokyo Shibaura Electric Co, Kawasaki, Japan*

*Received 20 May 1969*

The effect of particle size ( $0.78 \sim 4.4 \mu\text{m}$ ) on the sintering kinetics of AlN powder was investigated in the temperature range from 1600 to 2000° C and the results were analysed on the basis of vacancy diffusion models. The mechanisms of sintering are discussed.

Fractional shrinkage is proportional to the  $n$ th power of soaking time with  $n = 0.20$  for 4.4  $\mu\text{m}$  and 1.5  $\mu\text{m}$  powders and 0.33 for 0.78  $\mu\text{m}$  powder. For the 0.78  $\mu\text{m}$  powder at 1900° C, however,  $n$  decreases gradually as grain growth proceeds. The experimental activation energy for sintering is between 92 kcal/mole for 4.4  $\mu\text{m}$  and 129 kcal/mole for 0.78  $\mu\text{m}$  powder. Unlike this activated energy, the rate of sintering and the diffusion constant calculated from it increase drastically with decrease of particle size; the derived diffusion constant for 1.5  $\mu\text{m}$  powder is  $10^1$  to  $10^2$  times larger than that of 4.4  $\mu\text{m}$  powder, and for 0.78  $\mu\text{m}$  powder the diffusion constant is estimated to be still higher.

The particle-size dependence of parameter  $n$  and the diffusion constant seems to be caused by a variation in predominant diffusion mechanisms; namely, bulk diffusion in coarse powder and surface or grain-boundary diffusion in fine powder.

## 1. Introduction

Aluminium nitride (AlN) sublimates at 2450° C without liquefying under normal (non-oxidising) pressure [1]. Excellent properties of the material at high temperature, namely, high thermal conductivity, high electrical resistance, low thermal expansion, and high resistance against corrosion by acids and molten metals make AlN products very useful for high-temperature chemical, metallurgical, electrical and vacuum technologies [2-6]. However, sufficiently dense and strong AlN products for commercial uses have not been obtained to date by the sintering technique. This resembles the cases of silicon carbide and silicon nitride.

Long and Foster [3] tried to make AlN rods by high pressure moulding and high temperature ( $\sim 2000^\circ\text{C}$ ) sintering of AlN powder. The density and strength of the products, however, were not sufficient for practical uses. Taylor and Lenie [2] made dense AlN products by hot-pressing. But the technique is not convenient for mass production of articles with complicated shapes.

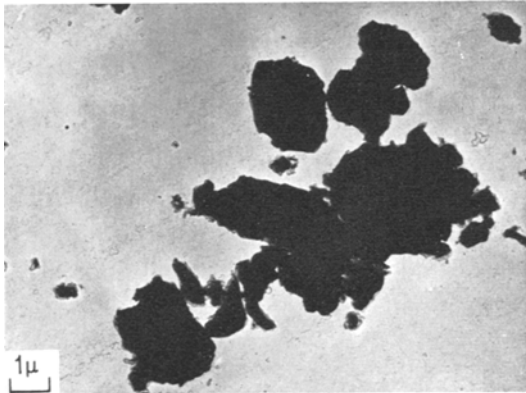
Recently, we found that dense, strong sintered products could be obtained from fine AlN powder and that the rate of sintering was strongly influenced by the particle size of the raw powder. Processes for manufacturing sintered articles were described in a previous paper [7]. As far as the authors know, the kinetics and sintering mechanisms of the material have not previously been studied. This paper describes the particle-size dependence of the kinetics and includes a discussion of the mechanisms of sintering.

## 2. Experimental Method

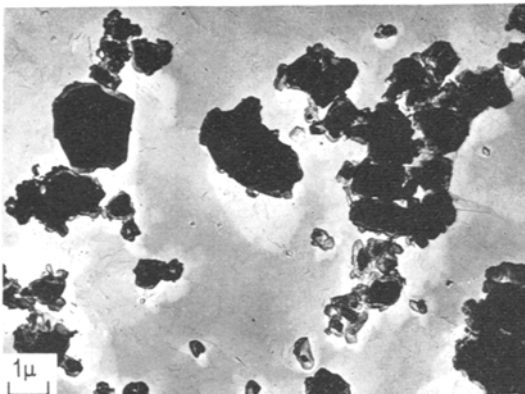
A mixture of aluminium powder and AlN powder (4:6 in weight ratio) was heated in a nitrogen atmosphere at 700° C. As the nitriding reaction of Al is exothermic, the temperature of the reacting system rose spontaneously [8]. The system was kept reacting for 1 h.

Three lots of raw powder were prepared by ball-milling the reaction product for varied times. The average particle diameters measured by Fisher's Subsieve Sizer were 4.4, 1.5 and 0.78  $\mu\text{m}$ .

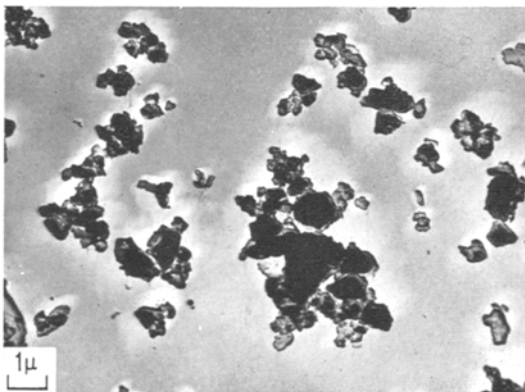
Electron micrographs of the particles are shown in fig. 1, and the results of spark emission spectrographic analysis are represented in table I.



(a)



(b)



(c)

Figure 1 Electron micrographs of raw powders: (a) 4.4  $\mu\text{m}$ ; (b) 1.5  $\mu\text{m}$ ; (c) 0.78  $\mu\text{m}$ ; in average diameter.

TABLE I Results of spark emission analysis of three lots of raw powders.

Particle size, $\mu\text{m}$	4.4	1.5	0.78
Impurity, ppm			
B	10-30	10-30	3-10
Si	300-1000	1000-3000	1000-3000
Fe	300-1000	300-1000	300-1000
Mn	30-100	10-30	10-30
Mg	10-30	10-30	30-100
V	10-30	10-30	10-30
Cu	30-100	10-30	3-10
Ti	10-30	10-30	10-30
Ca	3-10	3-10	10-30
Ba	—	3-10	3-10

Sample rods 8 mm in diameter and 15 mm in length were formed from each raw powder by pressing in a mould. Fifteen parts of paraffin was added as binder to 100 parts of raw powder (in weight ratio). Each rod was placed in an AlN crucible with AlN powder around it. The crucible was inserted in an electric furnace with a tubular carbon heater. Nitrogen gas was flowed through the furnace at the rate of 800 l/h. Samples were first heated to 300° C quickly and then heated slowly for 4 h to 400° C to expel the binder. After these preliminary heat-treatments, they were heated to the final sintering temperature at the rate of 60° C/min. Temperature and time of sintering were between 1600 and 2000° C and between 10 and 240 min. Preliminary experiments showed that sintering was very slow below 1500° C while AlN decomposed or vaporised rapidly at temperatures over 2100° C.

The sample temperature was measured with an optical pyrometer through holes in the crucible, heater and furnace wall (fig. 2). Diameters of the rods before and after sintering ( $L_0$  and  $L$ , respectively) were measured by means of a micrometer. Fractional shrinkage,  $(L_0 - L)/L_0$ , is plotted in figs. 3 and 4.

### 3. Results

Isothermal time-shrinkage curves for three lots of raw powder are shown in fig. 3. At constant soaking temperature, the samples shrank comparatively rapidly in the early stage and then slowly in the later stage of sintering. Total shrinkage increased with increase of temperature and with decrease of raw powder particle size. Electron micrographs of some of the sintered masses are shown in fig. 5.

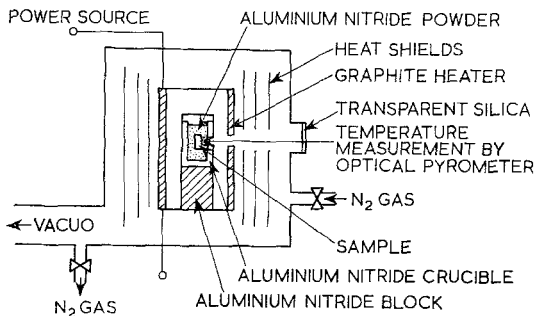


Figure 2 Schematic sketch of the furnace used for sintering samples.

#### 4. Discussion

Log time/log shrinkage plots (fig. 4) lead to the following experimental equation:

$$(\Delta L/L_0) = Kt^n$$

Here,  $\Delta L$  is  $(L_0 - L)$ ,  $t$  is time and  $K$  and  $n$  are constants. Values of the parameter  $n$  thus obtained are represented in table II. Values of  $n$  for 4.4 and 1.5  $\mu\text{m}$  powders are about 0.20, while, for 0.78  $\mu\text{m}$  powder,  $n$  is about 0.33 at 1700 and 1800° C and about 0.20 at 1900° C.

A possible interpretation of these results is as follows: in the finest powder, the predominant

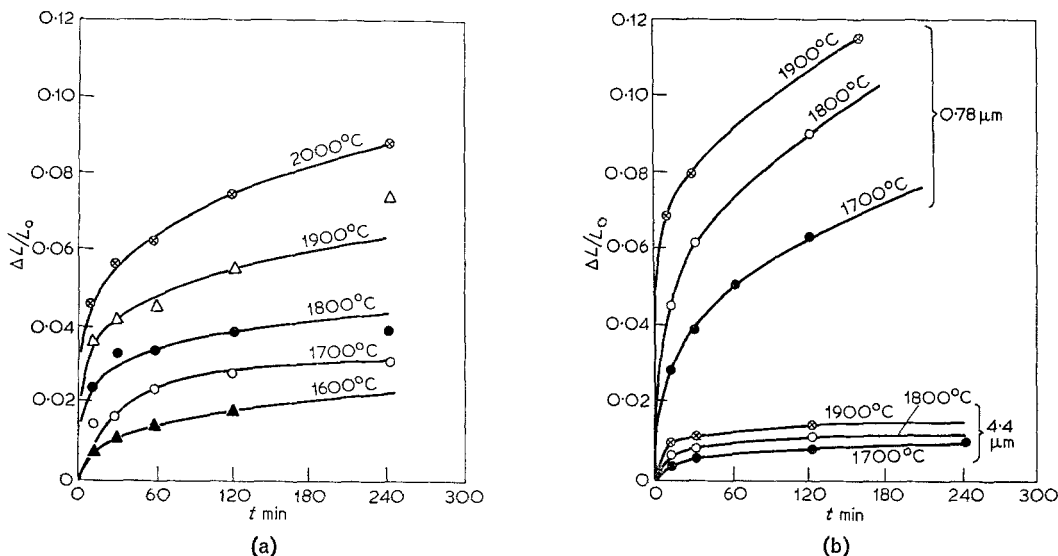


Figure 3 Isothermal shrinkage-time curves for three lots of raw powders. (a) 1.5  $\mu\text{m}$ ; (b) 4.4 and 0.78  $\mu\text{m}$ .

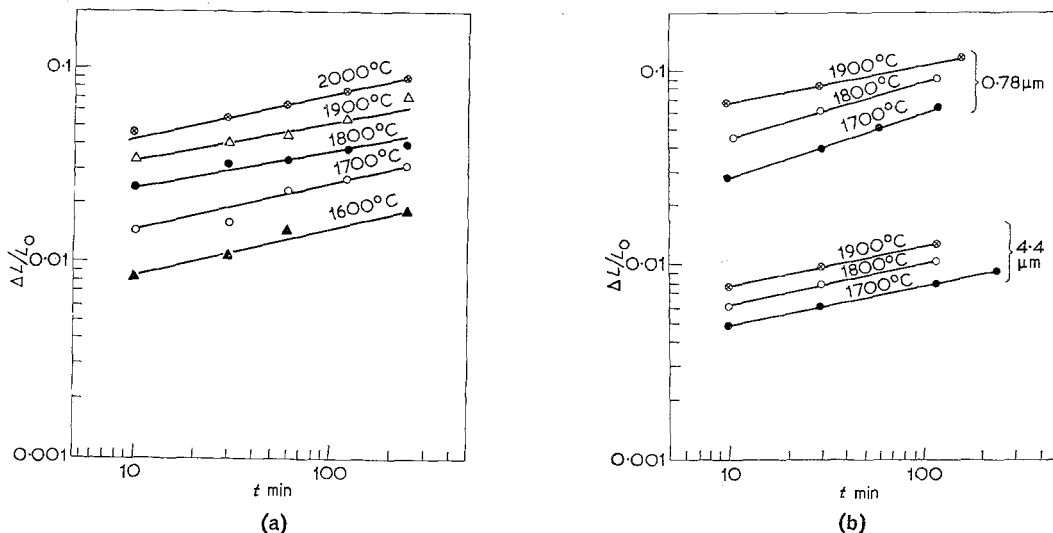


Figure 4 Isothermal shrinkage-time curves plotted on a logarithmic scale for three lots of raw powders. (a) 1.5  $\mu\text{m}$ ; (b) 4.4 and 0.78  $\mu\text{m}$ .

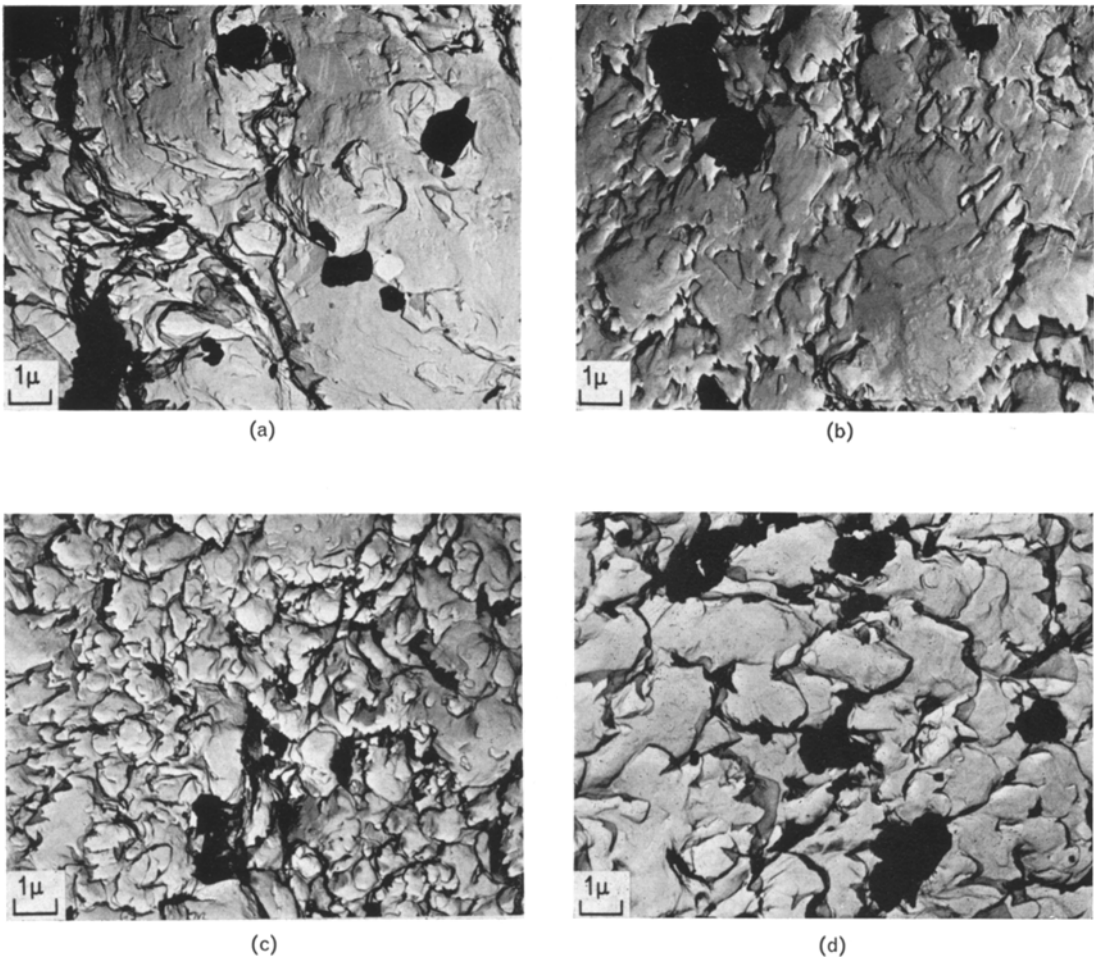


Figure 5 Electron micrographs of some raw powders. (a) Sintering of 4.4  $\mu\text{m}$  powder for 10 min at 1700° C. (b) Sintering of 4.4  $\mu\text{m}$  powder for 120 min at 1700° C. (c) Sintering of 0.78  $\mu\text{m}$  powder for 10 min at 1700° C. (d) Sintering of 0.87  $\mu\text{m}$  powder for 120 min at 1700° C.

TABLE II Values of  $n$  in equation 1 derived from figs. 3 and 6.

Particle size, $\mu\text{m}$	Sintering temperature, °C	$n$	$\bar{n}$
4.4	1700	0.189	0.196
	1800	0.200	
	1900	0.200	
1.5	1600	0.227	0.219
	1700	0.244	
	1800	0.200	
	1900	0.208	
	2000	0.218	
0.78	1700	0.333	0.328
	1800	0.323	
	1900	0.193	

diffusion mechanism which governs the process of sintering differs from those for the other powders, resulting in a high value of  $n$  (about 0.3); at 1900° C, however, distinct shrinkage and grain growth occurs in the early stage of sintering and slows down the compaction in the later stage, making  $n$  apparently identical with  $n$ 's for coarser powders. Electron micrographs (fig. 5) indicate marked grain growth of the finest powder at 1900° C and thus confirm this view. Slowing down of shrinkage caused by grain growth was already reported by Alexander and Balluffi [9] in their investigation on the sintering of copper.

Assuming that the sintering process proceeds through vacancy diffusion in the system, caused

by differences between the equilibrium concentrations of vacancies at neck surface and grain-boundary, we can introduce equations which represent the kinetics of sintering [10-13].

By analogy with surface tension or vapour pressure of a liquid drop, the equilibrium concentration of vacancies at the surface of a grain is assumed to be a linear function of  $(1/R_1 + 1/R_2)$  where  $R_1$  and  $R_2$  are principal radii of curvature at the point under consideration. Therefore, the difference between the vacancy concentration  $\Delta C$  at the neck ( $R_1 = \rho$ ,  $R_2 = -x$ ) and at the centre of a grain-boundary ( $R_1 = R_2 = \infty$ ), is represented by the following equation:

$$\frac{\Delta C}{C_0} = \frac{\gamma a^3}{kT} \left( \frac{1}{\rho} - \frac{1}{x} \right).$$

Here,  $C_0$  = equilibrium vacancy concentration at the centre of a grain-boundary;  $\gamma$  = surface free energy;  $a^3$  = volume of each vacancy;  $k$  = Boltzman constant;  $T$  = absolute temperature;  $x$  and  $\rho$  = principal radii of neck surface parallel and perpendicular to grain boundary surface, respectively.

Usually

$$\frac{1}{\rho} \gg \frac{1}{x}$$

and, as a result,

$$\frac{\Delta C}{C_0} \approx \frac{\gamma a^3}{kT\rho}.$$

The difference in vacancy concentration drives the vacancies to diffuse according to Fick's law, and causes counter-diffusion of the constituent atoms of the material through the bulk of the grains (volume diffusion) or along grain-boundaries to the neck surface. Sintering or shrinkage of the system then proceeds according to the following equation [12]:

$$\frac{\Delta L}{L} = \left( \frac{K\gamma a^3 D}{kTr^p} \right)^n t^n.$$

Here,  $D$  = effective or apparent diffusion coefficient of constituent atoms;  $r$  = particle radius;  $K$  = constant which depends on temperature;  $p$  = constant which depends on mechanism and path of diffusion. Parameters in the above equation, obtained by many investigators, are summarised in table III.

The values and particle size dependence of  $n$  represented in table II strongly suggest that in the sintering of the finest AlN powder, grain-

TABLE III Values of  $n$  in equation 2 obtained by previous investigators for various diffusion models.

Diffusion path	$n$	$P$	References
Bulk	0.46	3	[12]
Bulk	0.40	3	[11]
Bulk	0.50	3	[13]
Grain-boundary	0.31	4	[12]
Grain-boundary	0.33	4	[13]

boundary diffusion is predominant; in coarser powders it is hindered by the other slower and less efficient diffusion mechanisms. This view is also supported by consideration of the apparent diffusion coefficient, described below.

Assuming an experimental temperature dependence for  $K$ , the values of the activation energy  $Q$ , of sintering, are obtained from fig. 6, with results listed in table IV.  $Q$  is not greatly dependent on particle size and the very rapid sintering of the finest powder cannot be attributed to particle size dependence of  $Q$ .

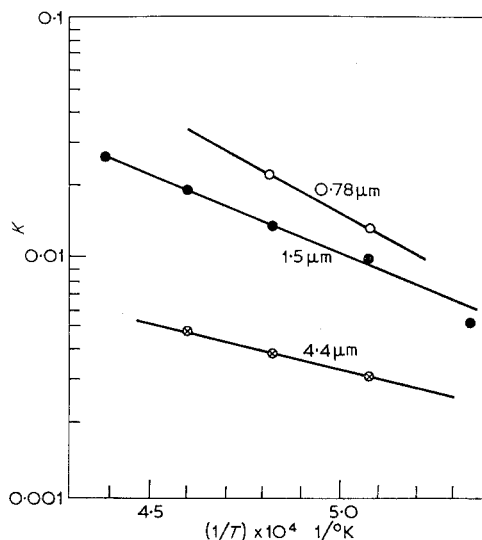


Figure 6 Parameter  $K$  plotted on a logarithmic scale against the reciprocal of absolute temperature for three lots of raw powders.

For the diffusion constant  $D$ , on the other hand, things are somewhat different;  $D$  strongly depends on particle size. For example, at  $1700^\circ\text{C}$ , assuming the other parameters to be equal, the ratio  $(D \text{ for } 1.5 \mu\text{m powder}) / (D \text{ for } 4.4 \mu\text{m powder})$  is in the range  $10^1$  to  $10^2$ .

The particle size dependence of the diffusion

TABLE IV Particle size dependence of experimental activation energy.

Particle size $\mu\text{m}$	4.4	1.5	0.78
Experimental activation energy (kcal/mole)	$92 \pm 5$	$107 \pm 5$	$129 \pm 5$

constant seems to be attributable to a change in the predominant diffusion mechanisms; namely from bulk diffusion with a lower diffusion constant in coarser grains to surface or grain-boundary diffusion with a higher constant in finer grains. As reported by previous investigators, surface or grain-boundary diffusion constants are generally higher than those of bulk diffusion. Diffusion of carbon into tantalum [14] and self-diffusion in sintering of metallic particles [10] are some examples for which this is true.

The authors intend to verify this view by radio-tracer experiments in the future.

## 5. Conclusions

The rate of sintering of AlN powder depends markedly on particle size; the rate increases with decrease of the particle size.

Fractional shrinkage is proportional to the  $n$ th power of sintering time with  $n$  between 0.2 and 0.33.  $n$  is about 0.2 for 4.4  $\mu\text{m}$  and 1.5  $\mu\text{m}$  powders and 0.33 for 0.78  $\mu\text{m}$  powder.  $n$  for the 0.78  $\mu\text{m}$  powder, however, decreases with grain growth at 1900° C to about 0.20.

The experimental activation energy of sintering is between 92 kcal/mol for 4.4  $\mu\text{m}$  powder and 129 kcal/mol for 0.78  $\mu\text{m}$  powder; it is not markedly dependent on particle size, and thus, particle size dependence of the energy cannot be the cause of the rapid sintering of fine powder.

The diffusion constant determined from the

sintering rate, on the other hand, strongly depends on the particle size; the diffusion constant for 1.5  $\mu\text{m}$  powder is  $10^1$  to about  $10^2$  times larger than that for 4.4  $\mu\text{m}$  powder, and for 0.78  $\mu\text{m}$  powder, the diffusion constant is estimated to be still higher.

The particle size dependences of the parameter  $n$  and the diffusion constant seem to have their origin in the difference in predominant diffusion mechanisms; namely, bulk diffusion in coarse powder, and grain-boundary or surface diffusion in fine powder. This explains the formation of dense and strong sintered products from fine AlN powder.

## References

1. TH. RENNER, *Z. anorg. Chem.* **298** (1958) 22.
2. K. M. TAYLOR and C. LENIE, *J. Electrochem. Soc.* **107** (1960) 308.
3. G. LONG and L. M. FOSTER, *J. Amer. Ceram. Soc.* **42** (1959) 53.
4. *Idem*, *Am. Ceram. Soc. Bull.* **40** (1961) 423.
5. S. MATSUO, K. KOMEYA, and Y. MATSUKI, *J. Ceram. Assoc. Japan* **73** (1965) 82.
6. G. A. COX, D. O. CUMMINS, K. KAWABE, and R. H. TREDGOLD, *J. Phys. Chem. Solids* **28** (1967) 543.
7. K. KOMEYA and H. INOUE, *J. Ceram. Assoc. Japan* **77** (1969) 136.
8. S. MATSUO, K. KOMEYA, and Y. MATSUKI, *ibid* **75** (1967) 241.
9. B. H. ALEXANDER and R. W. BALLUFFI, *Acta Met.* **5** (1957) 666.
10. G. C. KUCZYNSKI, *Trans. AIME* **185** (1949) 169.
11. W. D. KINGERY and M. BERG, *J. Appl. Phys.* **26** (1955) 1205.
12. D. L. JOHNSON and J. M. CUTLER, *J. Amer. Ceram. Soc.* **46** (1963) 541.
13. R. L. COBLE, *ibid* **41** (1958) 55.
14. H. SUZUKI, U. KIMURA, and S. HASE, "Symposium on High Temperature Materials" Tokyo, Japan (1968).